Włodzimierz Bednarek
dr hab. inż.
Politechnika Poznańska
Wydział Budownictwa i Inżynierii Środowiska
Zakład Budowy Mostów i Dróg Kolejowych
włodzimierz.bednarek@put.poznan.pl

DOI: 10.35117/A_ENG_20_02_02

Longitudinal displacements of railway jointless track due to local temperature difference on its length

Abstract: In the paper is shown an analysis of a CWR track's longitudinal displacements due to a local temperature difference on its length. The thermical forces on the railway track length arise due to a local temperature difference of rail, causing the local, zonal the longitudinal displacements of rail cross-sections. Axial displacements of track induce in succession a longitudinal reaction of roadbed in such a degree on which a arising displacements allow. Additionally a arising during track operating a variable longitudinal resistance on track's length (generated among other things by different state of ballast compaction, different pressure force of rail foot to divider), periodical acting force from vehicles, different value of adhesion wheels with rails and also different stage of rail heating, cause a disturbance section of equilibrium state of CWR track. In certain cases it assumes a shape of rails micro displacements, which can take a form e.g. creep displacements leading to value changes of longitudinal forces on this segment length with arising displacements. In paper analytical form of considered problem is given and computational examples, diagrams and tables reflecting influence of analyzed parameters on obtained a CWR track's longitudinal displacements due to local temperature difference on its length is inserted

Keywords: CWR track; Longitudinal displacement; Local temperature difference

Introduction

The problem of longitudinal displacements of a railway track finds its application in the analysis of various problems during its operation (e.g. assessment of the railway surface due to permanent longitudinal displacements, the interaction of the bridge with the track under conditions of temperature changes, stability or track lifting in the vertical plane [1-5, 7, 9-11,15,16]). The problem analyzed in the study is related to the local segments of the occurrence of horizontal displacements of the rail cross-sections, which are a consequence of the actual non-uniform temperature distributions occurring in them along the length of the jointless track [5,8,12,17]. We also encounter the phenomenon under consideration in the zones of horizontal longitudinal displacements of the jointless track, in its extreme sections (within the so-called *breathing sections*). Horizontal displacements of the *u* track due to temperature changes, in turn, cause a horizontal reaction of the ballast substrate *r(u)*, depending on the value of the shift *u* of the track cross-section (Fig. **1**). In the literature on railways, various characteristics of the longitudinal resistance of the road bed can be found [16]:

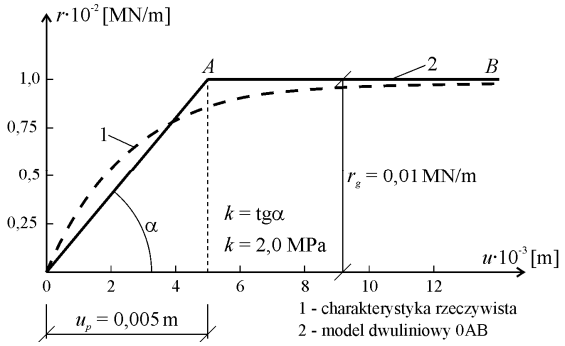

1. Typical longitudinal resistance during operation (wooden base) [16]
1) actual research; 2) two-line model
where: k – theoretical coefficient of horizontal stiffness of the substrate [MPa];
u_p – displacement value signaling a change in the soil resistance model

The real resistance of the ballast substrate is described by a substitute model, most often by an elastic, plastic, or elastic-plastic model [1,3,4] - Fig. **2**. The substitute models are used to analyze e.g. longitudinal displacements due to local temperature difference or train braking [7,8,12].

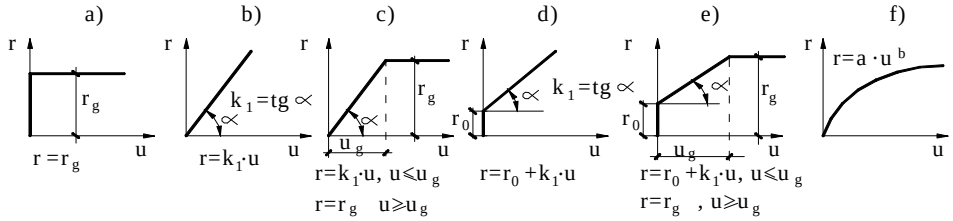

2. Models of longitudinal resistance of the ballast substrate adopted designations (used for calculations in the work): r_g – limit ballast substrate resistance [MN/m];
k_1 – the coefficient of horizontal stiffness of the substrate [MPa]; u_g – displacement limit that signals a change model of ballast substrate resistance [m]; r_0 – the initial resistance of the ballast substrate [MPa]

For the model of plastic resistance of the ballast substrate (model $r = r_g$ from Fig. 2a), we can write down the average cumulative resistance in the form [6]:

$$r_{sr} = \frac{N_t}{l_0}, \tag{1}$$

where: N_t – thermal force in the track, $N_t = \alpha_t \cdot E_S \cdot A \cdot \Delta t$, [kN];

α_t – rail steel expansion coefficient, [1/°C]; $E_S \cdot A$ – longitudinal stiffness of the track, [MN];

Δt – rail temperature rise, [°C];

l_0 – length of the loosened section of the track when adjusting the stresses, [m],
is the displacement of a loosened rail end (δ) can be formulated [6]:

$$\delta = \alpha_t^2 \cdot E_S \cdot A \cdot \frac{\Delta t^2}{2 \cdot r_{sr}} \tag{2}$$

and the extension of the free end of the rail can be formulated as below:

$$\delta = \int_{l_0}^{0} \lambda \cdot \Delta t \; dl = \lambda \cdot l_0 \cdot \Delta t = C_1 \cdot \Delta t, \tag{3}$$

where: $\lambda = 0{,}5 \cdot \alpha_t = 6 \cdot 10^{-6}$ [6], for $\alpha_t = 1.2 \cdot 10^{-5} \left[1/{}^{o}C \right]$

Using these formulas we get:

$$\alpha_t^2 \cdot E_S \cdot A \cdot \frac{\Delta t^2}{2 \cdot r_{sr}} = C_1 \cdot \Delta t \;\Rightarrow\; \alpha_t \cdot N_t \cdot \frac{\Delta t}{2 \cdot r_{sr}} = C_1 \cdot \Delta t \;\Rightarrow\; r_{sr} = \frac{\alpha_t}{2 \cdot C_1} \cdot N_t \tag{4}$$

where: C_1 is a characteristic quantity of a given track surface condition [6].

Finally, by additionally introducing an auxiliary parameter C_r (cumulative longitudinal resistance constant), longitudinal resistance can be formulated as follows [6]:

$$C_1 = \sum_{i=1}^{n} \frac{1}{n} \cdot \left(\frac{\frac{\delta_i}{2}}{\Delta t} \right), \; C_r = \frac{\alpha_t^2 \cdot E_S \cdot A}{2 \cdot C_1^2} \text{ and } r_{sr} = C_r \cdot \delta . \tag{5}$$

Table **1** shows the characteristics of longitudinal resistance for a jointless track made of rails 60E1 (based on experimental studies [6]):

Tab. 1. Dependence of the average cumulative resistance on the condition of the alloy screws

The condition of the alloy screw	Thermal time constant of the track $C_1\ [mm/1°C]$	Cumulative longitudinal constant resistance $C_r\ [MN/m^2]$	Section length l_0 [m]	r_{sr} $[MN/m]$
1	**2**	**3**	**4**	**5**
twisted properly	**0,3272**	**1,0614**	54,4872	**0,00902**
twisted properly	**0,2885**	**1,3634**	48,0770	**0,01023**
70% loosed	**0,8077**	**0,1739**	134,6154	**0,00365**
all loosed	**1,3847**	**0,0592**	230,7692	**0,00213**

As it results from the tab. 1 for correctly tightened alloy screws, the resistance of the ballast substrate is $r_0 = r_{sr} \approx 0{,}002 \div 0{,}01\,[MN/m]$ (values adopted for calculation examples). Using formulas 4 and 5 in Figs. **3** ÷ **5**, the following dependencies are presented: the cumulative longitudinal resistance constant from the thermal constant of the track, the longitudinal ballast resistance to rail displacements for different temperatures and the displacements of the loosened rail from temperature.

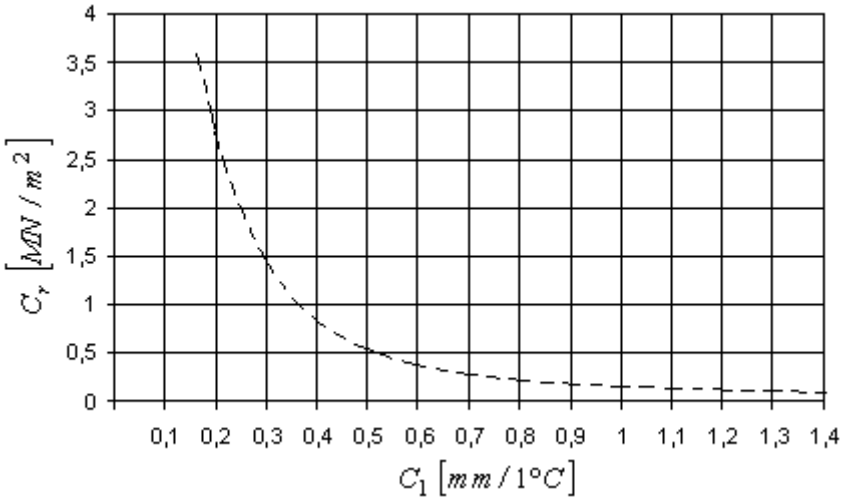

3. Dependence of the cumulative longitudinal resistance constant on the track thermal constant

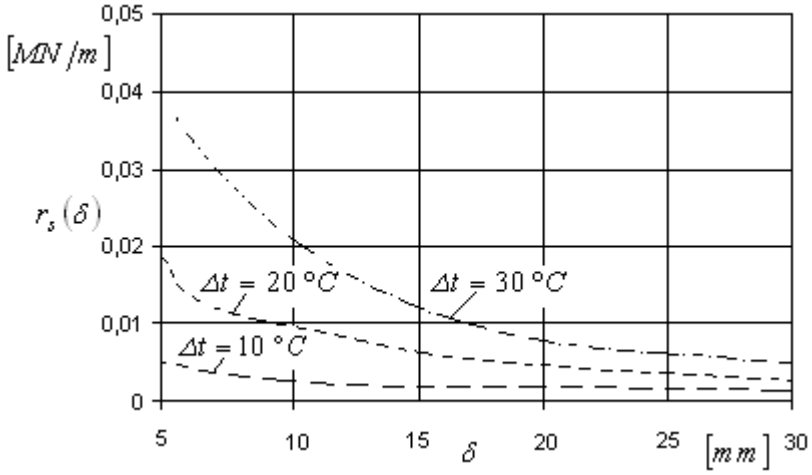

4. Dependence of ballast longitudinal resistance on rail displacements for different temperatures

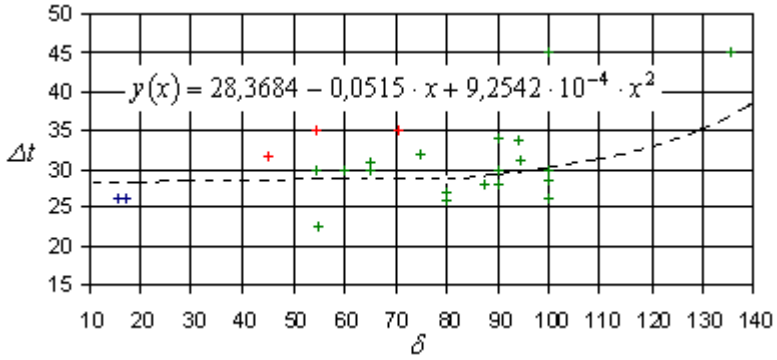

5. Dependence of displacements of a loosened rail on temperature [6]

The dependencies and values obtained at this point were used for the calculation examples presented in Fig. 10 and in Table 2 and 3.

Uneven temperature distribution along the length of the jointless railway track

The temperature of the rails depends on many variables. The main ones are natural, such as air and ground temperature, ground humidity, the intensity of solar radiation, cloudiness, transparency of the atmosphere, wind strength and direction, etc. In general, there is a dependency between the rail temperature and the air temperature (Fig. **6**) (measured at the same place and time), which can be represented as a relation: $t = t_0 + \tilde{t}_z$, where: t - rail temperature, t_0 - air temperature, and $\tilde{t}_z$ - variable random value, dependent in the period of high temperatures mainly on the intensity of insolation of the track.

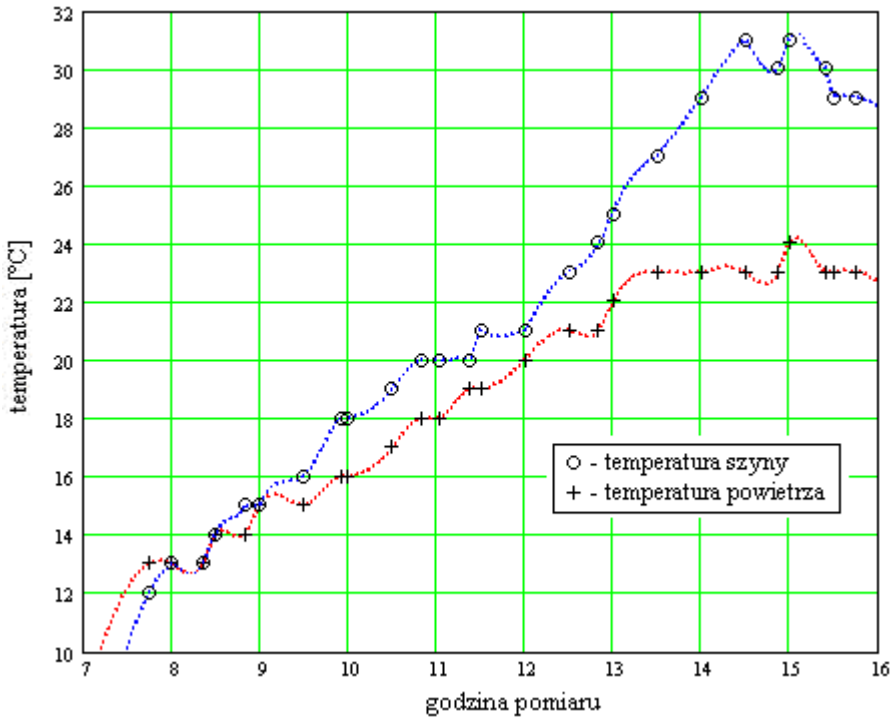

6. Dependence of rail and air temperature on the time of measurement (own research)

In the field operating conditions of the jointless track, there are uneven distribution of rail temperatures, both along the length of the track and in its cross-section (the measured temperature difference between the head and the foot of the rail can be as high as 7 [°C]).

The variable temperature difference occurring then in the track cross-sections: $\Delta t = t - t_P$, causes an uneven longitudinal distribution in the real jointless track. Considering the phenomenon of local zones of horizontal displacements of the jointless track due to uneven temperature distributions of the rails *t*, one should also take into account, apart from the longitudinal resistance of the ballast, variable along the length of the ballast, variable thermal conditions occurring during the assembly of the track, which are generally characterized by a variable temperature attaching rails to thermal sleepers $N_t = E_S \cdot A \cdot \alpha_t \cdot \Delta t$, the course of which is shown schematically with a solid line in Fig. 7. This unevenness is additionally increased by the influence of creep of the operated jointless track under train traffic, which causes unfavorable changes in the t_P temperature system. The dashed line in Fig. **7** shows the design **thermal force distribution** N_{t0}. For the N_{t0} distribution in the central part of *CD* $\left(N_{t0} = const.\right)$ we have *u=0* (no longitudinal displacements - stationary segment). Whereas *u=0* (parabola 2 °) occurs on the so-called moving (breathing) l_r long sections, where N_{t0} has a linear distribution ($r = r_g$,Fig. 2a). The computational N_{t0} (trapezoidal) distribution in Fig. 7 corresponds to a special case of the behavior of a straight jointless track with a uniform temperature increase along its entire length, for t_p=const.

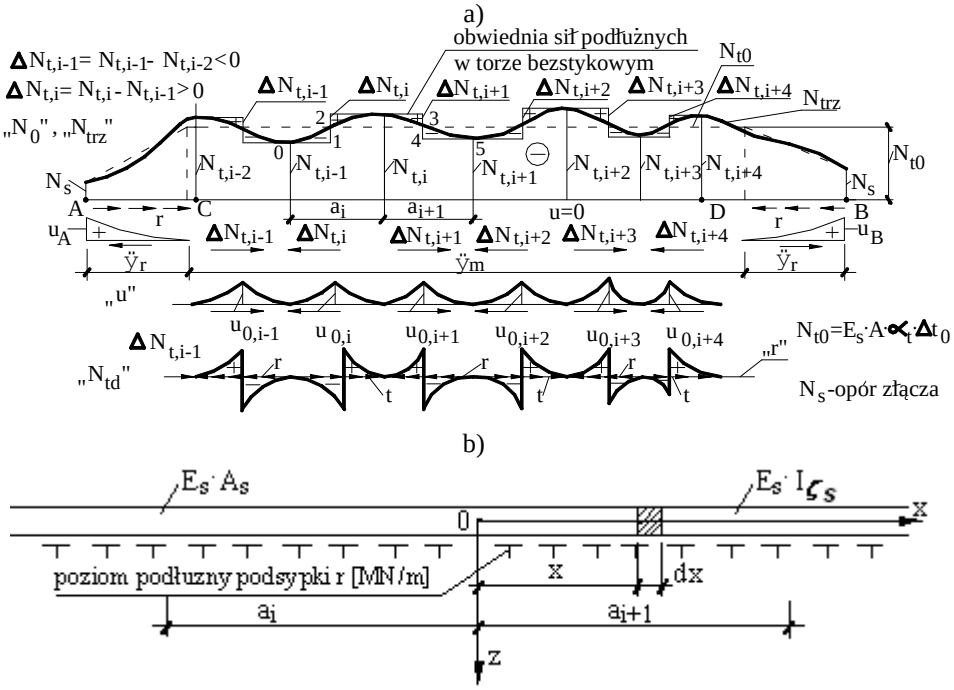

7. Distribution of thermal force along the length of a jointless railway track
a) uneven distribution of thermal force (N_{trz}) along the length of a jointless railway track and longitudinal movements of the track (u) and additional thermal force (N_{td});
b) the resulting longitudinal resistance of the bedding substrate (r) and bending stiffness ($E_sI_{\zeta s}$) and transverse (E_sA_s) railroad track

The state of axial displacements in the jointless track due to the influence of local temperature changes

The forces ΔN occurring as a result of local temperature differences of the rail along the track, shown schematically in Fig. **7**, cause local, zone-wide horizontal displacements of the rail cross-sections with maximum values from $u_{0,i-1}$ to $u_{0,i+4}$ [1,3,4,11]. The axial displacements of the track induce the horizontal reaction of the subsoil *r(u)* to the extent that the value of *u* allows. The function *r(u)*, for the purposes of the analysis, can be described using several models shown in Fig. **2**.

For example, consider the impact of force $\Delta N_{ti} = N_{t,i} - N_{t,i-1} = E_S \cdot A \cdot \alpha_t \cdot (\Delta t_i - \Delta t_{i-1})$ on the track operation, assuming $r=r_g$ most unfavorably (model from Fig. 2a). We will then obtain the formulas for u, N_{td} and l_w (computational schemes and the approximate course of the functions u and N_{td},, in the local system, are shown in Fig. **8**):

$$u = \frac{r_g}{2 \cdot E_S \cdot A} \cdot x^2 - \frac{\Delta N_{ti}}{2 \cdot E_S \cdot A} \cdot x + \frac{\Delta N^2{}_{ti}}{8 \cdot E_S \cdot A \cdot r_g} \tag{6}$$

$$N_{td} = r_g \cdot x - \frac{\Delta N_{ti}}{2},\ l_w = \frac{\Delta N_{ti}}{2 \cdot r_g}. \tag{7}$$

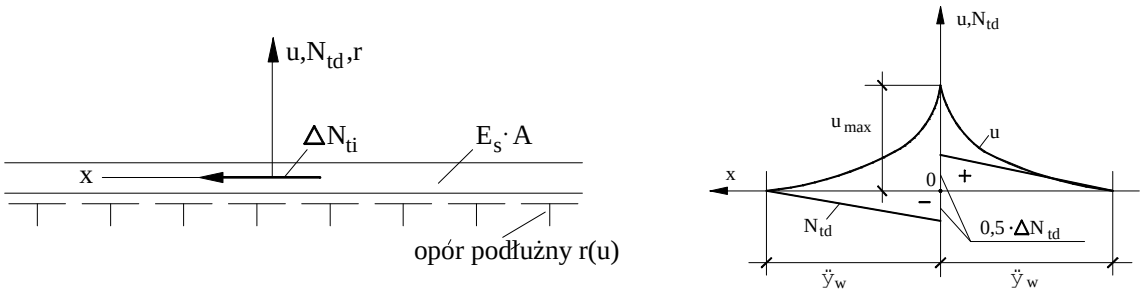

8. Calculation scheme and functions *u* (longitudinal displacement) and N_{td} (additional thermal force

For the elastic model from Fig. 2b, with $r = k_1 \cdot u$, we have:

$$u = \frac{\Delta N_{ti}}{2 \cdot E_S \cdot A \cdot \sqrt{\alpha}} \cdot e^{-\sqrt{\alpha} \cdot x},\ N_{td} = -\frac{\Delta N_{ti}}{2} \cdot e^{-\sqrt{\alpha} \cdot x},\ l_w = \infty \text{ and } \alpha = \frac{k_1}{E_S \cdot A}. \tag{8}$$

In turn, for the model from Fig. 2d, with $r = r_0 + k_1 \cdot u$, we obtain:

$$u = -\frac{\beta}{\alpha} \cdot \left[1 - cosh\left(\left(\sqrt{\alpha} \cdot x \right) \mp arcsin\, h\left(\frac{\Delta N_{ti} \cdot \sqrt{\alpha}}{2 \cdot \beta \cdot E_S \cdot A} \right) \right) \right], \tag{9}$$

$$N_{td} = \frac{\beta \cdot E_S \cdot A}{\sqrt{\alpha}} \cdot \left[sinh\left(\left(\sqrt{\alpha} \cdot x \right) \mp arcsin\, h\left(\frac{\Delta N_{ti} \cdot \sqrt{\alpha}}{2 \cdot \beta \cdot E_S \cdot A} \right) \right) \right], \tag{10}$$

$$l_w = \frac{1}{\sqrt{\alpha}} \cdot arcsin\, h\left(\frac{\Delta N_{ti} \cdot \sqrt{\alpha}}{2 \cdot \beta \cdot E_S \cdot A} \right), \text{ where: } \alpha = \frac{k_1}{E_S \cdot A},\ \beta = \frac{r_0}{E_S \cdot A}, \tag{11}$$

k_1 – the coefficient of the horizontal stiffness of the substrate [MPa].

Determination of parameters of longitudinal resistance for calculations

In the operated railway track, the actual values, e.g. k_1 and r_0 for model *d* $\left(r = r_0 + k_1 \cdot u\right)$ the elastic-plastic resistance of the road bed substrate from Fig. 2 is unknown. For certain boundary conditions [14] and taking into account the *d* model from Fig. 2, we get :

$$u(x) = -\frac{\alpha}{\beta} \cdot \left[1 - cosh\left(\sqrt{\alpha} \cdot x - arcsin\, h\left(\frac{\alpha_t \cdot \Delta t \cdot \sqrt{\alpha}}{\beta} \right) \right) \right], \tag{12}$$

where: $\alpha = \frac{k_1}{E \cdot A_s}$, $\beta = \frac{r_0}{E \cdot A_s}$, x – the abscissa of any section of the track, measured from the end of the jointless track under consideration. Using the results of direct measurements of the u^p axial displacements of the jointless track, it is possible to provide a method of their calculation (using the least-squares method) [14]:

$$\sum_{j=1}^{m} \sum_{i=1}^{n} V_{ji}^2 = min, \text{ where: } V_{ji} = u_{ji}(x) - u_{ji}^p, \tag{13}$$

whereas:

$u_{ji}(x) = F_{ji}\left(x_i, \Delta t_j, \alpha, \beta\right)$ denotes the displacements calculated for the pre-estimated values k_1 and r_0, so α_0 and β_0,

u_{ji}^p denotes the corresponding measured quantities $u_{ji}(x)$,

$j = 1,2,...m$ means another difference Δt, for which the value of the function (12) is determined and the measurement is made u_{ji}^p and $i = 1,2,...,n$ marks the place of measurement, i.e. the abscissa of a selected selected rail section (Fig. **9**).

9. Measurement of the longitudinal displacement of a railway track depending on temperature (author's photo)

The differences V_{ji} result mainly from the changes in the longitudinal resistance of the substrate along the track and from measurement errors. Using the equation (13), the unknown corrections $\delta(\alpha)$ and $\delta(\beta)$ are calculated and in subsequent iteration steps, up to the assumed approximation error . As a result of the calculations it is obtained: $\alpha = \alpha_0 + \sum \delta(\alpha)$ and $\beta = \beta_0 + \sum \delta(\beta)$, which provide the most precisely defined longitudinal resistance characteristic for a given railway track.

In the work [14] on the experimental training ground of a jointless railway track on the Katowice-Kraków railway line, the following values were obtained:

$$\boxed{r_0 = 9{,}728 \cdot 10^{-4} \pm 2{,}883 \cdot 10^{-4}\ [MN/m]} \text{ and } \boxed{k_1 = 1{,}8976 \pm 0{,}1589\ [MN/m^2]}.$$

Confirmation of these values is shown in Fig. 1.

Examples of calculation

Therefore, the following data was used for the calculations:

- jointless track 49E1 and 60E1, with wooden sleepers, on track ballast, in a local arrangement (Fig. 8), with the values of [1,3-5,13,16]:
- $E_S \cdot A = 2644{,}74\ MN$ (49E1); $E_S \cdot A = 3228{,}12\ MN$ (60E1) and:
- $\alpha_t = 1{,}15 \cdot 10^{-5}\ \frac{1}{K}$, $r_0 = 0{,}003\ MN/m$, $r_g = 0{,}010\ MN/m$,
- $k_1 = 1{,}0\ MPa$, $k_1 = 1{,}4\ MPa$ and $k_1 = 2{,}0\ MPa$ with $u_g = 0{,}005\ m$ (see Fig. 1 and Fig. 2),
- $\Delta(\Delta t)_i = 1, 2, \ldots, 14\,[K]$.

In order to illustrate the obtained maximum track displacements, Fig. **10** shows the calculation results for the parameters adopted above and the models described in Figs. **1** and **2** of this paper.

a)

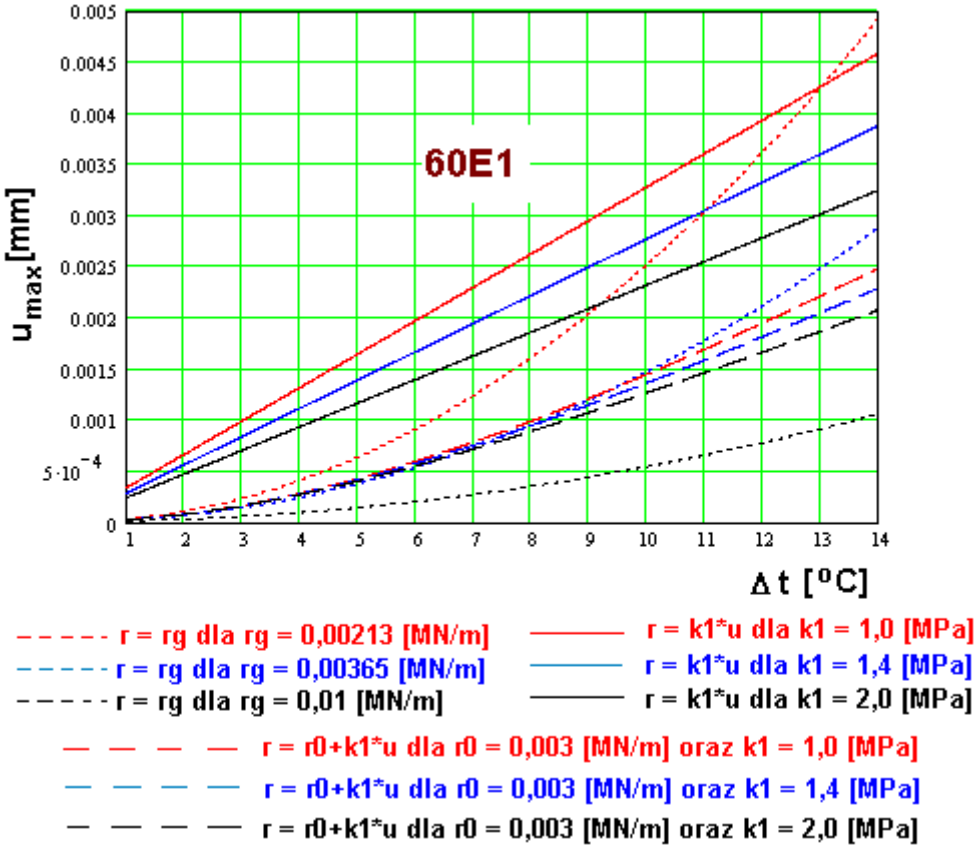
60E1
u_{max} [mm]
0.005
0.0045
0.004
0.0035
0.003
0.0025
0.002
0.0015
0.001
$5 \cdot 10^{-4}$
0
1 2 3 4 5 6 7 8 9 10 11 12 13 14
Δ t [°C]
r = rg dla rg = 0,00213 [MN/m]
r = rg dla rg = 0,00365 [MN/m]
r = rg dla rg = 0,01 [MN/m]
r = k1*u dla k1 = 1,0 [MPa]
r = k1*u dla k1 = 1,4 [MPa]
r = k1*u dla k1 = 2,0 [MPa]
r = r0+k1*u dla r0 = 0,003 [MN/m] oraz k1 = 1,0 [MPa]
r = r0+k1*u dla r0 = 0,003 [MN/m] oraz k1 = 1,4 [MPa]
r = r0+k1*u dla r0 = 0,003 [MN/m] oraz k1 = 2,0 [MPa]

b)

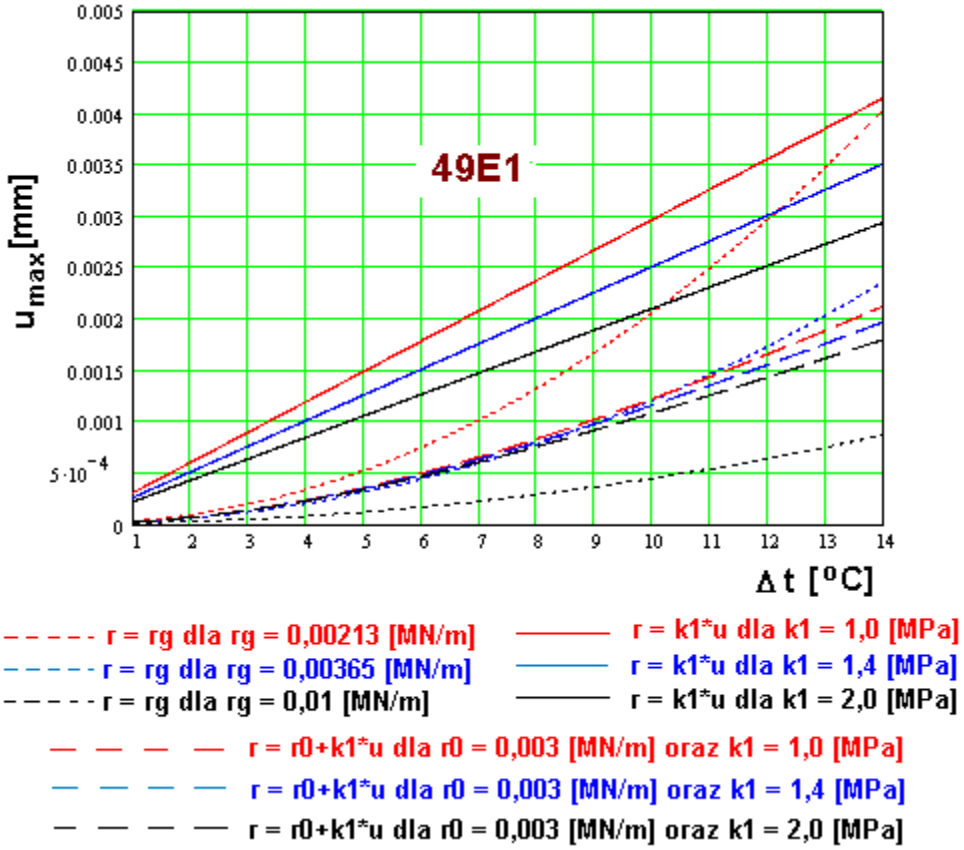

10. Maximum track displacements due to local temperature difference Δ(Δti)for the adopted calculation models (formulas 6-11)
a) track with rails 60E1; b) track with 49E1 rails
(Δti)

As shown in Fig. 10, the smallest displacements are obtained for the plastic model with the assumed highest resistance value (r_g=0,01 [MN/m]). However, the largest displacements are obtained for the elastic model with the adopted lowest resistance value (k_1=1,0 [MPa]). This should be explained by the properties of the analyzed models (Fig. 2). For the plastic model, from the very beginning of the track displacement, the longitudinal resistance of the road bed (r=r_g) arises, while for the elastic model, this resistance increases only with the resulting displacement.

In order to show the differences arising from the adopted models (Fig. 2), calculations were made with the following data:
jointless track **60E1**, with wooden sleepers, on ballast bedding, in a local arrangement (Fig. 8) and:

$E_S \cdot A = 3228\ MN$, $\alpha_t = 1{,}15 \cdot 10^{-5}\ \frac{1}{K}$, $r_0 = 0{,}003\ MN/m$, $r_g = 0{,}010\ MN/m$,

$k_1 = 1{,}4\ MPa$, $u_g = 0{,}005\ m$. In addition, it was assumed: $\Delta(\Delta t)_i = 7{,}0\ K$, where:

$$\Delta(\Delta t)_i = \frac{\Delta N_{ti}}{E_S \cdot A \cdot \alpha_t},$$

whereas $\Delta N_{ti} = N_{ti} - N_{t,i-1} = E_S \cdot A \cdot \alpha_t \cdot (\Delta t_i - \Delta t_{i-1})$,

$\Delta t_i = t_i - t_{pi} - t_s$, $\Delta t_{i-1} = t_{i-1} - t_{p,i-1} - t_s$, t – the rail temperature, t_p – the temperature of the attached rail to the sleepers, $t_S = \frac{N_S}{E_S \cdot A \cdot \alpha_t}$, N_S – the horizontal reaction of the rail contact to thermal influences, $\left(N_S \cong 0{,}20\ MN\right)$, $\Delta(\Delta t)_i = \Delta t_i - \Delta t_{i-1} = \left(t_i - t_{i-1}\right) - \left(t_{pi} - t_{p,i-1}\right)$.
Hence, $\Delta N_{ti} = E_S \cdot A \cdot \alpha_t \cdot \Delta(\Delta t)_i = 0{,}26\ MN$. The calculation results are shown in tab. **2**:

Tab. 2. Longitudinal displacements *u(x)*, distribution of thermal force *Nt(x*) and transverse resistance *r(x)* depending on the adopted calculation model

1° – for the model from Fig. 2a ($r = r_g$) we obtain:	**2°** – for the model from Fig 2b ($r = k_1 \cdot u$) we obtain:	**3°** – for the model from Fig 2d ($r = r_0 + k_1 \cdot u$) we obtain:
1	**2**	**3**
$u = 1{,}55 \cdot 10^{-6} \cdot x^2 \mp 4{,}03 \cdot 10^{-5} \cdot x + 2{,}62 \cdot 10^{-4}$ for: $x > 0, (-),\ x < 0, (+)$. For $x = 0$, $u_{\max} = 2{,}62 \cdot 10^{-4}\ m$ with $u_g = 5{,}0 \cdot 10^{-3}\ m$ and $N_{td} = 0{,}01 \cdot x \mp 0{,}130$, $x > 0, (-),\ x < 0\ (+)$ $l_w = 13{,}0\ m$ $r = r_g = -E_S \cdot A \cdot \frac{d^2u}{dx^2} = -0{,}01\ MN/m$	$\alpha = \frac{k_1}{E_S \cdot A} = 4{,}337 \cdot 10^{-4}\ m^{-2}$, $\sqrt{\alpha} = 2{,}0826 \cdot 10^{-2}\ m^{-1}$ $u = 1{,}934 \cdot 10^{-3} \cdot \exp(\mp 2{,}0826 \cdot 10^{-2} \cdot x)$ for $x > 0, (-),\ x < 0, (+)$. For $x = 0$: $u_{\max} = 1{,}934 \cdot 10^{-3}\ m$ with $u_g = 5{,}0 \cdot 10^{-3}\ m$ $r = -E_S \cdot A \cdot \frac{d^2u}{dx^2} = -k_1 \cdot u =$ $= -2{,}708 \cdot 10^{-3} \cdot exp(\mp 2{,}0826 \cdot 10^{-2} \cdot x)$ for $x = 0$, $r_{\min} = -2{,}708 \cdot 10^{-3}\ MN/m$ $N_{td} = E_S \cdot A \cdot \frac{du}{dx} = \mp 0{,}130 \cdot \exp(\mp 2{,}0826 \cdot 10^{-2} \cdot x)$ $l_w = \infty$, $\lim_{x \to \pm\infty} N_{td} = 0$, $\lim_{x \to \pm\infty} r = 0$	$\alpha = 4{,}337 \cdot 10^{-4}\ m^{-2}$, $\beta = \frac{r_0}{E_S \cdot A} = 9{,}2937 \cdot 10^{-7}\ m^{-1}$ $u = -2{,}143 \cdot 10^{-3} \cdot \left[1 - cosh\left(\begin{matrix} 2{,}0826 \cdot 10^{-2} \cdot x \mp \\ \mp\ arcsin\,h(0{,}9025) \end{matrix}\right)\right]$ for: $x > 0, (-),\ x < 0, (+)$ $u = -2{,}143 \cdot 10^{-3} \cdot \left[1 - \cosh(2{,}0826 \cdot 10^{-2} \cdot x \mp 0{,}8107)\right]$ for $x = 0$: $u_{\max} = -2{,}143 \cdot 10^{-3} \cdot (1 - 1{,}347) = 0{,}7436 \cdot 10^{-3}\ m$ with $u_g = 5{,}0 \cdot 10^{-3}\ m$ $N_{td} = E_S \cdot A \cdot \frac{du}{dx} = 0{,}144 \cdot \sinh(2{,}0826 \cdot 10^{-2} \cdot x \mp 0{,}8107)$ for $x = 0$: $N_{td} = \mp 0{,}13\ MN$ $l_w = 38{,}927\ m$; for $x = l_w$: $u = 0$, $N_{td} = 0$ $r = -E_S \cdot A \cdot \frac{d^2u}{dx^2} = -0{,}003 \cdot \cosh(2{,}0826 \cdot 10^{-2} \cdot x \mp 0{,}8107)$ for $x = \pm l_w$, $r = -0{,}003\ MN/m$ for $x = 0$, $r = -1{,}347 \cdot 0{,}003 = -0{,}00404\ MN/m$ $\omega = \int_0^{-l_w} r\,dx = 0{,}130\ MN$, $r_{śr} = -\frac{\omega}{l_w} = -0{,}00334\ MN/m$

Fig. **11** shows the curves of the calculated functions *r(x)* for the obtained values of I_w:

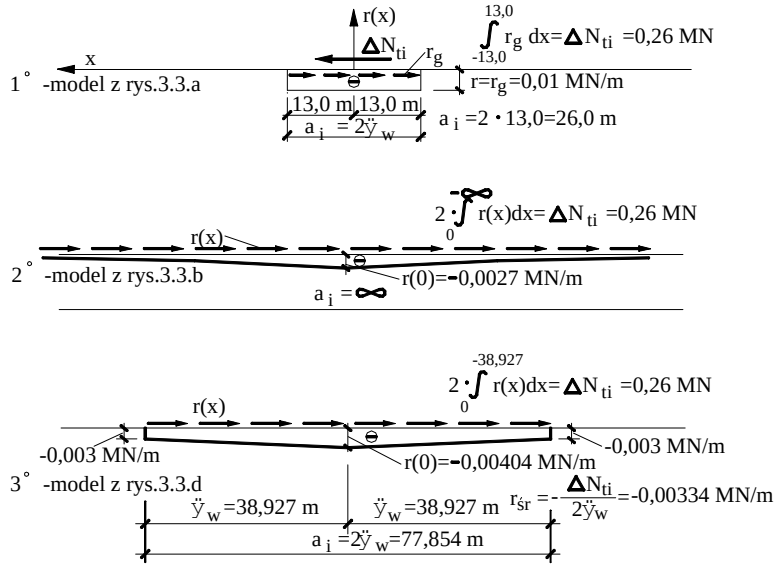

11. Distributions of functions r(x) for various computational models [2,3]

Discussion of the results

The usefulness of the applied soil models for the analysis of the axial displacements of the jointless track is different. For large temperature rises Δt, np. $\Delta t = 45\ K$, e.g. accompanied by high values of thermal force in the rails, the jointless track experiences significant axial shifts, greater than u_g, what takes place mainly in the so-called *breathable sections*, then the plastic model will prove useful (Fig.2a). On the other hand, for the analysis of the influence of local uneven temperature changes along the track length, the correct model for further application is the model of longitudinal resistance of the ballast from Fig. 2d. The usefulness of the elastic model (Fig. 2b), often used effectively in the field of e.g. the buckling analysis of the track in the vertical plane, is rather limited in the considered case of uneven temperature changes.

On the other hand, assuming for the calculations, for example, too high values of the coefficient of horizontal stiffness of the subgrade k_1=5÷10 [MPa], is not fully confirmed in the results of experimental tests of the longitudinal resistance of the ballast (see Fig. 12). Therefore, a reasonable compromise is to adopt the following parameter values: $r_0 = 0{,}003\ MN/m$, $r_g = 0{,}01 MN/m$, $k_1 = 2{,}0 MPa$, $u_g = 0{,}005\ m$, which are justified both in Fig. **2** and Fig. **12**:

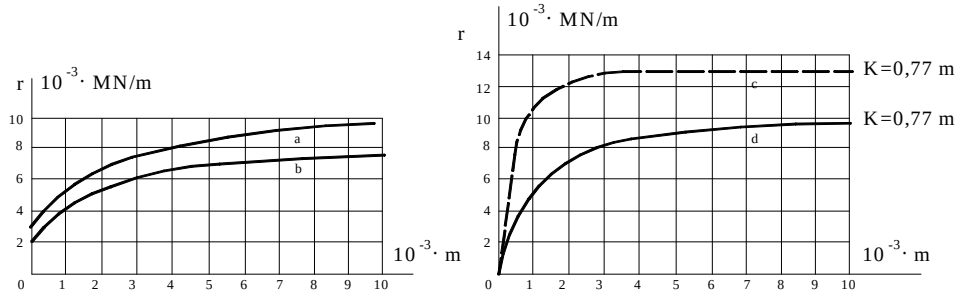

12. Experimental characteristics of the ballast longitudinal resistance [6]

a - longitudinal resistance with the spacing of wooden sleepers 65 cm (span 22 sleepers)

b - longitudinal resistance with the spacing of wooden sleepers 65 cm (span 11 sleepers)

c - longitudinal resistance with variable spacing of wooden sleepers (K-spacing of sleepers)

d - longitudinal resistance with a variable spacing of prestressed concrete sleepers (K-sleeper spacing)

For these parameters and the above-mentioned models (a, b and d) from Fig. **2** it is calculated:

Tab. 3. Longitudinal displacements $u(x)$, distribution of thermal force $N_t(x)$ and transverse resistance $r(x)$ depending on the adopted calculation model

1° – for the model from Fig. 2a ($r = r_g$) we obtain:	**2°** – for the model from Fig. 2b ($r = k_1 \cdot u$) we obtain:	**3°** – for the model from Fig. 2d ($r = r_0 + k_1 \cdot u$) we obtain:
1	**2**	**3**
for $\boldsymbol{r_g}$ = **0,002131** [MN/m] $\boxed{u = 3{,}31 \cdot 10^{-7} \cdot x^2 \mp 4{,}03 \cdot 10^{-5} \cdot x + 1{,}23 \cdot 10^{-3}}$ $u(0) = u^1_{max} = 1{,}23 \cdot 10^{-3} m;\ l_w = 61{,}0m$ for $\boldsymbol{r_g}$ = **0,00365** [MN/m] $\boxed{u = 5{,}65 \cdot 10^{-7} \cdot x^2 \mp 4{,}03 \cdot 10^{-5} \cdot x + 7{,}17 \cdot 10^{-4}}$ $u(0) = u^2_{max} = 7{,}17 \cdot 10^{-4} m;\ l_w = 35{,}62m$ for $\boldsymbol{r_g}$ = **0,01** [MN/m] $\boxed{u = 1{,}55 \cdot 10^{-6} \cdot x^2 \mp 4{,}03 \cdot 10^{-5} \cdot x + 2{,}62 \cdot 10^{-4}}$ $u(0) = u^3_{max} = 2{,}62 \cdot 10^{-4} m;\ l_w = 13{,}0m$ where for: $x > 0, (-), x < 0, (+)$ $u^3_{max} < u^2_{max} < u^1_{max} < u_g$ dla $u_g = 5{,}0 \cdot 10^{-3} m$ and respectively: $r = -E_S \cdot A \cdot \frac{d^2u}{dx^2} = r_g$ $N_{td} = r_g \cdot x - \frac{\Delta N_{ti}}{2}$ $x > 0, (-),\ x < 0, (+)$	for $\boldsymbol{k_1}$ = 2,0 [MPa] $\alpha = \frac{k_1}{E_S \cdot A} = 6{,}196 \cdot 10^{-4} m^{-2},\ \sqrt{\alpha} = 2{,}4891 \cdot 10^{-2} m^{-1}$ $\boxed{u = 1{,}618 \cdot 10^{-3} \cdot exp\left(\mp 2{,}4891 \cdot 10^{-2} \cdot x\right)}$ for $x > 0, (-),\ x < 0, (+)$. for $x = 0$: $u_{max} = 1{,}618 \cdot 10^{-3} m$ with $u_g = 5{,}0 \cdot 10^{-3} m$ $\boxed{\begin{aligned} r &= -E_S \cdot A \cdot \frac{d^2u}{dx^2} = -k_1 \cdot u = \\ &= -3{,}236 \cdot 10^{-3} \cdot exp\left(\mp 2{,}4891 \cdot 10^{-2} \cdot x\right) \end{aligned}}$ dla $x = 0$, $r_{min} = -3{,}236 \cdot 10^{-3} MN/m$ $N_{td} = E_S \cdot A \cdot \frac{du}{dx} = \mp 0{,}130 \cdot exp\left(\mp 2{,}4891 \cdot 10^{-2} \cdot x\right)$ $l_w = \infty,\ \lim_{x \to \pm\infty} N_{td} = 0,\ \lim_{x \to \pm\infty} r = 0$	for $\boldsymbol{k_1}$ = 2,0 [MPa] i $\boldsymbol{r_0}$ = 0,003 [MN/m] $\alpha = 6{,}196 \cdot 10^{-4} m^{-2},\ \beta = \frac{r_0}{E_S \cdot A} = 9{,}2937 \cdot 10^{-7}\ m^{-1}$ $\boxed{u = -1{,}5 \cdot 10^{-3} \cdot \left[1 - cosh\left(2{,}4891 \cdot 10^{-2} \cdot x \mp arcsin\,h(1{,}0786)\right)\right]}$ for: $x > 0, (-),\ x < 0, (+)$ $u = -1{,}5 \cdot 10^{-3} \cdot \left[1 - cosh\left(2{,}4891 \cdot 10^{-2} \cdot x \mp 0{,}9359\right)\right]$ $\boxed{u(0) = u_{max} = -1{,}5 \cdot 10^{-3} \cdot (1 - 1{,}471) = 0{,}7063 \cdot 10^{-3} m}$ for $u_g = 5{,}0 \cdot 10^{-3} m$ $N_{td}(x) = E_S \cdot A \cdot \left(\frac{\beta}{\sqrt{\alpha}} \cdot sinh\left(\sqrt{\alpha} \cdot x - a\,sinh\left(\frac{\Delta N_t}{2} \cdot \frac{\sqrt{\alpha}}{\beta \cdot E_S \cdot A} \right) \right) \right)$ $N_{td} = E_S \cdot A \cdot \frac{du}{dx} = 0{,}1205 \cdot sinh\left(2{,}4891 \cdot 10^{-2} \cdot x \mp 0{,}9359\right)$ dla $x = 0$: $N_{td} = \mp 0{,}13\ MN$ $l_w = 37{,}599m$; dla $x = l_w$ we have: $u = 0,\ N_{td} = 0$ $r = -E_S \cdot A \cdot \frac{d^2u}{dx^2} = -0{,}003 \cdot cosh\left(2{,}4891 \cdot 10^{-2} \cdot x \mp 0{,}9359\right)$ dla $x = \pm l_w$, $r = -0{,}003\ MN/m$ for $x = 0$, $r = -1{,}471 \cdot 0{,}003 = -0{,}004413 MN/m$ $\omega = \int_0^{-l_w} r\,dx = 0{,}130\ MN,\ r_{śr} = -\frac{\omega}{l_w} = -0{,}003475 MN/m$

Final conclusions:

Based on the performed analysis, it can be concluded that:

1) The analytical solution to the problem of the local temperature difference along the length of the jointless railway track presented in the paper showed the formation of its undesirable longitudinal displacements.
2) The theoretical analysis of factors causing longitudinal displacements of the track with the use of substitute calculation models of the actual characteristics obtained in the railway track (Fig. **2** or Fig. **12**) is presented.).
3) The calculation results presented in Fig. 10 show that the greatest displacement due to the temperature difference depends mainly on the temperature gradient and the parameters of the adopted calculation models (r_g, r_0 i k_1) and the track longitudinal stiffness ($E_S \cdot A$). Displacements resulting from uneven heating of the rail along its length (e.g. located in a shaded deep trench or exposed to solar insolation in an embankment) constitute a significant, underestimated part of the displacement, which may increase e.g. track creep
4) The significant influence of the analyzed models and the adopted parameters for calculations (r_g, r_0 i k_1) on the shape and values of longitudinal horizontal displacements of the railway track (Fig. 10) was indicated.
5) On the basis of the performed calculations and analyzes of the actual characteristics obtained in the railway track, appropriate parameters for the calculations were proposed (used in tables **2** and **3**).

Source materials

[1] Bednarek Wł.: *Practicability of longitudinal resistance models for effect analysis of local temperature change on axial displacement state in CWR track*. 13th International Conference on Modernisation of Railway tracks, Slovakia, Žilina, 2003,

[2] Bednarek Wł.: *Loss of contact analysis in jointless track on ballast due to influence of non-axial horizontal subsoil reaction transfer*. Archives of Civil Engineering, L, 3, 2004,

[3] Bednarek Wł.: *Influence of ballast longitudinal resistance on axial displacement state in CWR track due to local rail temperature changes*. Foundations of Civil and Environmental Engineering, Poznań University of Technology, No.12, 2008,

[4] Bednarek Wł.: *Wpływ oporu podłużnego podłoża podsypkowego na przemieszczenia osiowe bezstykowego toru kolejowego wskutek lokalnej różnicy temperatury*. Archiwum Instytutu Inżynierii Lądowej (Archives of Institute of Civil Engineering), Poznań University of Technology, Nr 11, 2011,

[5] Bednarek Wł.: *Wpływ pionowych odkształceń nawierzchni i podtorza na pracę toru bezstykowego*. Seria Rozprawy Nr 506, Wydawnictwo Politechniki Poznańskiej, Poznań 2013,

[6] Bogdaniuk B.: *Stateczność toru bezstykowego w procesie jego eksploatacji*. Praca doktorska, Poznań, 1972,

[7] Czyczuła Wł., Towpik K.: *Kryterium oceny nawierzchni kolejowej z uwagi na trwałe podłużne przemieszczenia szyn*. IX Krajowa Konferencja Naukowo-Techniczna „Drogi Kolejowe", Kraków, 1997,

[8] Czyczuła Wł., Towpik K.: *Problemy modelowania oraz identyfikacji modeli toru bezstykowego*. Problemy kolejnictwa, zeszyt 128, Warszawa, 1998,

[9] Dieterman H. A., Van M. A., Van Dam A. J. P., Esveld C.: *Longitudinal forces in railroad structures*. Rail Engineering International, No. 1, 1990,

[10] Frýba L.: *Distribution "quasi-statique" des forces de démarrage et de freinage dans les rails et les p*onts. Rail International, Février, 1975,

[11] Huber M. T.: *Pisma*. *Zagadnienia kolejowe*. Tom III, Dział VIII, PWN, Warszawa, 1957,
[12] Markine V., Esveld C.: *Analysis of longitudinal and lateral behaviour of a CWR track using a computer system LONGIN*. Delft University of Technology, 1999,
[13] PKP: Przepisy Id-1 (D-1) *Warunki techniczne utrzymania nawierzchni na liniach kolejowych*, Warszawa, 2005 z późn. zmianami,
[14] Szumierz W.: *Warunki stosowania torów bezstykowych na terenach ekaploatacji górniczej*. Temat 3001/16, 1972,
[15] Szumierz W.: *Statyka budowli liniowych poddanych działaniu sił poziomych od pełzania podłoża górniczego*. Główny Instytut Górnictwa, Katowice, 1980,
[16] Szumierz W., Stefanek J.: *Model współdziałania mostu z torem bezstykowym w warunkach zmian temperatury*. Drogi i Mosty, nr 2, 2004,
[17] Van M. A.: *Stability of continuous welded rail track*. Delft 1995.